

# Nonlinear Estimation of Cylindrically Symmetric Magnetic Susceptibility Anisotropy in Image Space Without a Rigid DTI Prior

Cynthia Wisnieff<sup>1</sup>, Pascal Spincemaille<sup>2</sup>, and Yi Wang<sup>1</sup>

<sup>1</sup>Cornell University, New York, New York, United States, <sup>2</sup>Weill Cornell Medical College, New York, New York, United States

**Target Audience** Anyone interested in white matter anisotropy

**Introduction:** Susceptibility tensor imaging (STI) can be reconstructed with both tensor orientation and cylindrical symmetry constraints on the tensor in k-space using diffusion tensor imaging (DTI) input, which is referred as k-space – Cylindrically Symmetric Susceptibility Tensor, k-CSST<sup>1-3</sup>. Tensor orientation constraints from DTI may be not be reliable due to biophysical differences between water diffusion around myelin sheath and susceptibility source from myelin sheath only and differing resolution with the gradient echo acquired STI data. We present here a technique that only imposes the cylindrical symmetry constraints.

**Theory: Nonlinear – Cylindrically Symmetric Susceptibility Tensor, nl-CSST:** The apparent susceptibility,  $\chi_a$ , at a given orientation of a cylindrically symmetric susceptibility tensor  $\chi = \text{diag}(\chi_{\parallel}, \chi_{\perp}, \chi_{\perp})$  is:  $\chi_a = (\chi_{\parallel} - \chi_{\perp})(\mathbf{f} \cdot \hat{\mathbf{b}})^2 + \chi_{\perp}$  Eq. 1, where  $\chi_{\parallel}$  and  $\chi_{\perp}$  are the susceptibility along and perpendicular to the axis of the cylinder,  $\mathbf{f}$  is the orientation of the fiber and  $\hat{\mathbf{b}}$  is the applied field direction. The magnetic susceptibility anisotropy is defined as  $\text{MSA} = \chi_{\parallel} - \chi_{\perp}$ .

## Methods:

**Phantom:** Carbon fiber sample in 1% agarose gel and two balloons filled with gadolinium, giving isotropic susceptibility of .81 and 1.62ppm respectively. Twelve orientations of the phantom were acquired evenly distributed over a sphere with 1mm<sup>3</sup> isotropic resolution of a multi-echo gradient echo(MEGRE) (TR/spacing/#Echoes) (71.6ms/3.4ms/8). **Human:** 12 MEGRE acquisitions (TR/spacing/#Echoes) (46.9ms/2.6ms/11) at 1.5mm<sup>3</sup> resolution+ 1 DTI acquisition were acquired on the same volunteer; 33 directions, b value of 1000s/mm<sup>2</sup> and 1 reference at a resolution of 2x2x2.4mm<sup>3</sup>. All data was collected on a GE 3T clinical scanner. **Image Reconstruction:** All twelve orientations were used for the reconstructions. In the k-CSST the tensor was estimated using a conjugate gradient solver<sup>2</sup>. In the nl-CSST the susceptibility anisotropy and the fiber orientation were estimated by solving Eq. 1 using a Levenberg-Marquardt solver using the diffusion direction as the initial guess and zero for the tensor components. Apparent susceptibility for each orientation was estimated using MEDI<sup>4</sup>.

## Results:

Phantom MSA images are shown on Fig.1 top. Estimates of MSA in the carbon fiber show nl-CSST(0.88± 0.42ppm) and k-CSST(0.74± 0.39ppm); differences that were not statistically significant, P>0.05.

Human MSA example images are shown in Fig.1 bottom row. Consistent MSAs were obtained for regions in the body (BCC) and splenium(SCC) of the corpus callosum and the optic radiations (OR) using both nl-CSST and k-CSST (Table 1).

## Discussion and Conclusion:

The nonlinear method permits imposing cylindrical symmetry without rigidly imposing a fiber orientation in the reconstruction. There was good agreement in estimated anisotropy between nl-CSST and k-CSST estimation in the carbon fiber phantom. In the volunteer there was a similar resemblance in the MSA maps of nl-CSST and k-CSST with greater sensitivity to noise in the nl-CSST. This increased noise sensitivity may be caused by the increased number of parameters in the estimation, which worsens the condition of the inverse problem, as well as the nonlinear algorithm. Despite sensitivity to noise, this method could provide further insight into the susceptibility anisotropy of more complex configurations of fibers. Differences between the estimated anisotropy from both methods needs to be further explored.

**References:**1. Li, X., et al., NeuroImage, 2012. 62(1): p. 314-30.2. Wisnieff, C., et al. *Feasible 3-Orientation Acquisition for Detecting Susceptibility Anisotropy in the Human Brain Using Prior Structural Information*. in *Proc. Intl. Soc. Mag. Reson. Med.* 2012. Melbourne. 3. Wharton, S. and R. Bowtell, *Proc. Intl. Soc. Mag. Reson. Med.*, 2011. 19: p. 4515.4. Liu, J., et al., NeuroImage, 2012. 59(3): p. 2560-8.

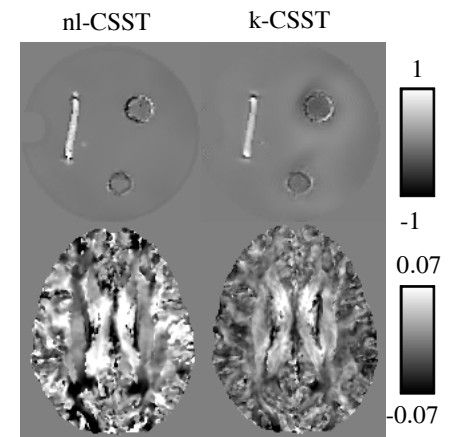


Fig. 1: MSA maps, in ppm, top row: Phantom Bottom row: Volunteer  
Table 1: Estimated MSA in the volunteer (ppb)

	nl-CSST	k-CSST
<b>SCC</b>	11.8±41.9	16.8±14.1
<b>BCC</b>	45.5±49.2	29.7±37.5
<b>OR</b>	7.7±32.2	6.5±16.7